Inorg. Chem. **1982**, *21*, 2661–2666

Contribution from the Departments of Chemistry, Texas A&M University, College Station, Texas 77843, and Tulane University, New Orleans, Louisiana 70118

X-ray Structural Studies of *cis*-$Mo(CO)_4(PR_3)_2$ (R = Me, Et, *n*-Bu) Derivatives and Their Relationship to Solution Isomerization Processes in These Octahedral Species

F. ALBERT COTTON,*[1] DONALD J. DARENSBOURG,*[2] S. KLEIN,[1] and BRIAN W. S. KOLTHAMMER[1]

Received November 5, 1981

The crystal and molecular structures of *cis*-$Mo(CO)_4(PMe_3)_2$ (**1**), *cis*-$Mo(CO)_4(PEt_3)_2$ (**2**), and *cis*-$Mo(CO)_4[P(n\text{-}Bu)_3]_2$ (**3**) have been determined for the purpose of seeking correlations between structural features—especially evidence of intramolecular strain—and reactivity. The main results are as follows. **1**: space group $P2_1/n$, with unit cell dimensions of $a = 9.770$ (1) Å, $b = 12.109$ (1) Å, $c = 14.183$ (1) Å, $\beta = 95.435$ (7)°, $V = 1670.5$ (5) Å^3, and $Z = 4$. The Mo–P distances average 2.522 (1) Å, and ∠P–Mo–P = 97.54 (4)°. **2**: space group $P2_1/c$, with unit cell dimensions of $a = 9.740$ (3) Å, $b = 16.399$ (1) Å, $c = 14.601$ (2) Å, $\beta = 109.49$ (2)°, $V = 2199$ (1) Å^3, and $Z = 4$. The Mo–P distances average 2.544 (4) Å, and ∠P–Mo–P = 100.27 (3)°. **3**: space group $P2_1/c$, with unit cell dimensions of $a = 20.27$ (1) Å, $b = 9.442$ (3) Å, $c = 19.011$ (6) Å, $\beta = 107.59$ (3)°, $V = 3468$ (4) Å^3, and $Z = 4$. The Mo–P distances average 2.552 (8) Å, and ∠P–Mo–P = 99.29 (4)°. Within this set of three compounds, there is a fairly good correlation of both steric strain, as evidenced by the P–Mo–P angles, and tendency to isomerize to the trans structure with the steric bulk of the PR_3 ligands as indicated by cone angles. However, comparison of structural variations in a total of seven *cis*-$Mo(CO)_4(PR_3)_2$ compounds shows that more subtle factors are also at work.

Introduction

This paper is a contribution to a continuing effort to clarify the relationship between structural properties (especially intramolecular steric interactions) and the reactivity in solution for the class of molecules represented generally by the formula *cis*-$M(CO)_4LL'$.[3–7] Particular attention has been focused on the *cis*-$Mo(CO)_4(PR_3)_2$ complexes, in which repulsive forces between the PR_3 ligands are often alleviated by isomerization to the corresponding trans species. Although neutral octahedral group 6B metal derivatives have generally been considered to be rather inert toward intramolecular, non-bond-breaking rearrangement processes, it appears that there are now several instances[4,8,9] where this isomerization reaction, e.g., (1), must follow an intramolecular, nondissociative course.

$$cis\text{-}Mo(CO)_4L_2 \underset{k_{-1}}{\overset{k_1}{\rightleftharpoons}} trans\text{-}Mo(CO)_4L_2 \qquad (1)$$

For example, where L = $P(n\text{-}Bu)_3$ or PEt_3 an intramolecular, nondissociative process was shown to occur on the basis of the lack of ^{13}CO incorporation into either *cis*- or *trans*-$Mo(CO)_4L_2$ or formation of $Mo(CO)_4(^{13}CO)L$ during the rearrangement process.[4] A trigonal rotation mechanism (eq 1, activation enthalpy = 24.5 kcal mol^{-1} or 102.5 kJ mol^{-1}) was used to account for these observations, where $k_1/k_{-1} = K_{eq} = 5.3$ for L = n-Bu_3P. This is to be compared with processes involving phosphine dissociation in derivatives of the type *cis*-$Mo(CO)_4L_2$, which occur with activation enthalpy of ~30 kcal mol^{-1}.

In order to extend the above observations to provide a comprehensive comparison of kinetic and structural features for a homologous series of compounds, we have measured the thermodynamic and kinetic data for reaction 1 when L = PMe_3 and carried out X-ray crystallographic structure determinations for all three of the *cis*-$Mo(CO)_4(PR_3)_2$ compounds, with R = Me, Et, and *n*-Bu.

Experimental Section

Compound Preparations. ***cis*-$Mo(CO)_4(PR_3)_2$ (R = Me, Et, *n*-Bu).** These complexes were prepared in their isomerically pure form by the published procedure.[4] *cis*-$Mo(CO)_4(NHC_5H_{10})_2$ (prepared from $Mo(CO)_6$ and excess piperidine in refluxing heptane) was stirred under reflux in dichloromethane with excess trialkylphosphine for 15 min (R = Et, *n*-Bu) or 1 h (R = Me). The reaction mixture was filtered through Celite, the filtrate reduced in volume, and methanol added to afford crystals of the desired products. The compounds were purified by recrystallization from cold methanol and vacuum-dried to provide crystals suitable for X-ray analysis.

Kinetic Measurements. The isomerization reaction of *cis*-$Mo(CO)_4(PMe_3)_2$ was carried out in a Schlenk storage tube (25-mL capacity) under an atmosphere of either nitrogen or carbon monoxide in heptane solvent. The tube was fitted with a septum cap secured by copper wire. The reaction flask was placed in a constant-temperature bath, and samples were withdrawn at regular time intervals with a hypodermic syringe for infrared spectral analysis. The rate of the *cis*-$Mo(CO)_4(PMe_3)_2$ → *trans*-$Mo(CO)_4(PMe_3)_2$ process and the equilibrium constant were determined as previously described[4] for the PEt_3 and $P(n\text{-}Bu)_3$ complexes.

Infrared Measurements. The infrared spectra were recorded in 1.0-mm matched NaCl sealed cells on a Perkin-Elmer 283B spectrophotometer equipped with an infrared data station and employing the PECDS software package provided by Perkin-Elmer. The spectra were calibrated against a water vapor spectrum below 2000 cm^{-1} and against a CO spectrum above 2000 cm^{-1}.

X-ray Diffraction Studies. Crystals of **1** and **2** were mounted on the end of thin glass fibers and examined on an Enraf-Nonius CAD-4 automated diffractometer. The automatic locating and centering of 25 reflections (26° ≤ 2θ ≤ 32°) followed by least-squares analyses of the setting angles produced accurate unit cell parameters (Table I), indicating monoclinic crystal systems. Peak profile analysis of several strong reflections for each crystal suggested the data collection parameters to be used (Table I). The space groups $P2_1/n$ and $P2_1/c$ for **1** and **2**, respectively, were uniquely determined by the observed systematic absences. Data were collected[10] in the range $0° < 2\theta \leq 50°$, and the data sets obtained were corrected for Lorentz and polarization effects. Absorption corrections were not made because of the low μ values for these crystals.

The structures were solved by standard heavy-atom methods, and the refinement[11] proceeded readily. In the case of **1**, a disorder of

---

[1] Texas A&M University.
[2] Tulane University.
[3] Darensbourg, D. J.; Kump, R. L. *Inorg. Chem.* **1978**, *17*, 2680.
[4] Darensbourg, D. J. *Inorg. Chem.* **1979**, *18*, 14.
[5] Darensbourg, D. J.; Graves, A. H. *Inorg. Chem.* **1979**, *18*, 1257.
[6] Cotton, F. A.; Darensbourg, D. J.; Klein, S.; Kolthammer, B. W. S. *Inorg. Chem.* **1982**, *21*, 1651.
[7] Cotton, F. A.; Darensbourg, D. J.; Klein, S.; Kolthammer, B. W. S. *Inorg. Chem.* **1982**, *21*, 294.
[8] Darensbourg, D. J.; Baldwin, B. J. *J. Am. Chem. Soc.* **1979**, *101*, 6447.
[9] Darensbourg, D. J.; Baldwin, B. J.; Froelich, J. A. *J. Am. Chem. Soc.* **1980**, *102*, 4688.
[10] Bino, A.; Cotton, F. A.; Fanwick, P. E. *Inorg. Chem.* **1979**, *18*, 3558.
[11] All crystallographic computing was performed on a PDP 11/60 computer at the Molecular Structure Corp., College Station, TX, with the Enraf-Nonius structure determination package.

0020-1669/82/1321-2661$01.25/0

Table I. Crystallographic Data

Enraf-Nonius CAD-4 (Used for 1 and 2)

	1	2
formula	$MoP_2O_4C_{10}H_{18}$	$MoP_2O_4C_{16}H_{30}$
mol wt	360.1	444.3
space group	$P2_1/n$	$P2_1/c$
a, Å	9.770 (1)	9.740 (3)
b, Å	12.109 (1)	16.399 (1)
c, Å	14.183 (1)	14.601 (2)
β, deg	95.435 (7)	109.49 (2)
V, Å^3	1670.5 (5)	2199 (1)
Z	4	4
d_{calcd}, g cm^{-3}	1.43	1.34
radiation	graphite-monochromated Mo Kα (λ = 0.710 73 Å)	
scan type	ω–2θ	ω–2θ
scan width ($\Delta\omega$), deg	0.65 + 0.35 tan θ	0.60 + 0.35 tan θ
no. of unique data	2927	3839
no. of data, $I > 3\sigma(I)$	2068	2756
p	0.05	0.05
no. of variables	181	298
R_1[a]	0.038	0.032
R_2[a]	0.053	0.042
esd	1.52	1.20
largest shift/error ratio[b]	0.29	0.40
largest peak[c]	0.20	0.22

Syntex P$\overline{1}$ (Used for 3)

formula	$MoP_2O_4C_{28}H_{54}$	a, Å	20.272 (10)
mol wt	612.6	b, Å	9.442 (3)
space group	$P2_1/c$	c, Å	19.011 (6)
Z	4	β, deg	107.59 (3)
d_{calcd}, g cm^{-3}	1.17	V, Å^3	3468 (4)
scan type	θ–2θ	scan rate, deg min^{-1}	2–24
no. of unique data	2059	no. of data, $I > 3\sigma(I)$	2023
no. of variables	316	R_1[a]	0.087
esd	2.67	R_2[a]	0.011
largest parameter shift[b]	0.18	largest peak[c]	0.66

[a] $R_1 = \Sigma|F_o| - |F_c|/\Sigma|F_o|$, $R_2 = [\Sigma w(|F_o| - |F_c|)^2/\Sigma w|F_o|^2]^{1/2}$. [b] Largest Δ_i/σ_i ratio in final refinement cycle. [c] Largest peak in a final difference Fourier, e Å^{-3}.

Table II. Final Positional Parameters for *cis*-$Mo(CO)_4(PMe_3)_2$

atom	x	y	z
Mo	0.56689 (4)	0.31156 (4)	0.22613 (3)
P(1)	0.6942 (1)	0.2357 (1)	0.0937 (1)
P(2)	0.3270 (2)	0.2642 (2)	0.1566 (1)
O(1)	0.4499 (5)	0.4109 (4)	0.4040 (3)
O(2)	0.8572 (4)	0.3751 (5)	0.3205 (3)
O(3)	0.5778 (7)	0.0794 (4)	0.3286 (4)
O(4)	0.5350 (6)	0.5446 (4)	0.1252 (3)
C(1)	0.4893 (6)	0.3749 (5)	0.3371 (4)
C(2)	0.7511 (6)	0.3524 (5)	0.2852 (4)
C(3)	0.5760 (7)	0.1626 (6)	0.2908 (4)
C(4)	0.5485 (6)	0.4616 (5)	0.1606 (4)
C10	0.7776 (9)	0.3428 (6)	0.0252 (5)
C11	0.6114 (8)	0.1486 (8)	−0.0028 (5)
C12	0.8404 (7)	0.1471 (6)	0.1377 (5)
C20	0.2747 (14)	0.3239 (13)	0.0402 (9)
C21	0.1891 (12)	0.3142 (17)	0.2192 (11)
C22	0.2867 (14)	0.1227 (10)	0.1326 (14)
C23	0.2151 (19)	0.3829 (20)	0.1642 (32)
C24	0.2464 (23)	0.1593 (23)	0.2273 (20)
C25	0.2770 (23)	0.2243 (31)	0.0391 (15)

Table III. Final Positional Parameters for *cis*-$Mo(CO)_4(PEt_3)_2$

atom	x	y	z
Mo	0.20120 (3)	0.03381 (2)	0.26126 (2)
P(1)	0.3094 (1)	0.15747 (6)	0.36521 (7)
P(2)	−0.0673 (1)	0.07281 (6)	0.20142 (7)
O(1)	0.1165 (4)	−0.1317 (2)	0.1503 (2)
O(2)	0.5151 (3)	−0.0345 (2)	0.3040 (3)
O(3)	0.2386 (4)	0.1243 (2)	0.0795 (2)
O(4)	0.1762 (4)	−0.0472 (2)	0.4525 (2)
C(1)	0.1431 (4)	−0.0698 (2)	0.1894 (3)
C(2)	0.4027 (4)	−0.0068 (3)	0.2921 (3)
C(3)	0.2227 (4)	0.0917 (2)	0.1440 (3)
C(4)	0.1843 (4)	−0.0177 (2)	0.3838 (3)
C110	0.4061 (5)	0.2314 (3)	0.3144 (3)
C111	0.5410 (5)	0.1991 (4)	0.2959 (4)
C120	0.1939 (5)	0.2263 (3)	0.4069 (3)
C121	0.1129 (6)	0.1846 (4)	0.4651 (4)
C130	0.4488 (5)	0.1269 (3)	0.4791 (3)
C131	0.5270 (7)	0.1938 (3)	0.5485 (4)
C210	−0.1828 (4)	0.0224 (3)	0.2621 (4)
C211	−0.1850 (5)	−0.0688 (3)	0.2546 (5)
C220	−0.1280 (4)	0.1790 (2)	0.2010 (3)
C221	−0.0656 (5)	0.2361 (3)	0.1436 (4)
C230	−0.1521 (5)	0.0440 (3)	0.0731 (4)
C231	−0.3127 (6)	0.0606 (4)	0.0237 (4)

one PMe_3 group was observed and a suitable model with identical weightings of two possible rotations (two sets of methyl carbon atoms) for this group was found. During the final stages of refinement of the structure of **2**, hydrogen atom positions were obtained from a difference map. These positions were refined as hydrogen atoms with fixed thermal parameters chosen as 1 + B_{iso}(av) (where B_{iso}(av) is the average isotropic thermal parameter for the α and β carbon atoms). The final refinement parameters for both structures are presented in Table I, and the discrepancy indices used are defined by

$$R_1 = \sum|F_o| - |F_c|/\sum|F_o| \qquad R_2 = [\sum w(|F_o| - |F_c|)^2/\sum w|F_o|^2]^{1/2}$$

The crystallographic study of **3** was greatly hampered by the low melting point of this complex (31 °C). Crystals could not be examined visually or photographically at room temperature. Hence, numerous crystals were examined on a Syntex P$\overline{1}$ four-circle automated diffractometer, which resides in a cold room held at 3 °C. All crystals diffracted reasonably well but produced rather broad peaks. Finally a large crystal, 0.3 × 0.3 × 0.5 mm, was selected that produced well-defined (albeit broad) peaks. Lattice parameters were obtained by a least-squares analysis of the setting angles for 15 strong reflections. Intensity data were collected[12] with use of graphite-monochromated Cu Kα radiation and θ–2θ scan rates varying from 2 to 24° min^{-1} depending on the intensity of the reflection. The range collected was $0° < 2\theta \leq 50°$. Background measurements were made at both limits of each scan. Three standard reflections were measured after every 97 data points. The systematic absences suggested the space group $P2_1/c$, and of the 2087 reflections collected, 2059 were unique. Only the reflections having intensities (I) greater than $3\sigma(I)$ were retained as observed (2023 data) and, after correction for Lorentz and polarization effects, were used to solve the structure. Two further corrections were also made to this data set during the initial stages of refinement. A consideration of the variation in intensity of the three standard reflections with time demonstrated that during the 52 h of data collection a linear decrease in intensity to the extent of 10% had occurred. A linear decay correction was then made to the data set using the parameters obtained from the intensity standard plot. Also, because of the high absorption coefficient of the crystal, an absorption correction was made using an empirical method based on ψ scans for χ values near 90°. The maximum, minimum, and average transmission factors were 0.99, 0.64, and 0.84, respectively.

The structure was solved by standard heavy-atom methods and refined to convergence with use of anisotropic thermal parameters for the Mo, P, O, and C atoms. The final discrepancy indices were R_1 = 0.087 and R_2 = 0.111, and the error in an observation of unit weight was 2.66. The largest shift/error ratio on the last cycle was 0.13. A final difference synthesis showed peaks up to 0.66 e Å^{-3} randomly distributed throughout the coordination sphere. All of these factors indicate that the model used for refinement is representative of the structure of **3** and that the large thermal and goodness of fit parameters are attributable to the low melting point of the compound.

Final positional parameters for compounds **1**–**3** are listed in Tables II–IV, respectively. All thermal vibration parameters, positional and thermal parameters of the hydrogen atoms in compound **2**, C–C distances in compounds **2** and **3**, and the structure factors are available as supplementary material.

---

[12] Cotton, F. A.; Frenz, B. A.; Deganello, G.; Shaver, A. *J. Organomet. Chem.* **1973**, *50*, 227.

Table IV. Final Positional Parameters for *cis*-$Mo(CO)_4[P(n\text{-}Bu)_3]_2$

atom	*x*	*y*	*z*
Mo	0.25176 (5)	0.1420 (1)	0.24770 (5)
P(1)	0.2372 (2)	−0.0172 (4)	0.3500 (2)
P(2)	0.2615 (2)	−0.0479 (4)	0.1554 (2)
O(1)	0.2647 (5)	0.3674 (9)	0.1344 (5)
O(2)	0.2488 (5)	0.3975 (9)	0.3495 (5)
O(3)	0.4145 (5)	0.1451 (11)	0.3126 (6)
O(4)	0.0888 (5)	0.1686 (11)	0.1821 (5)
C(1)	0.2603 (6)	0.284 (1)	0.1760 (6)
C(2)	0.2509 (6)	0.302 (1)	0.3135 (7)
C(3)	0.3545 (6)	0.139 (1)	0.2886 (6)
C(4)	0.1495 (6)	0.158 (1)	0.2036 (5)
C110	0.2063 (6)	−0.200 (1)	0.3321 (6)
C111	0.1374 (7)	−0.209 (1)	0.2791 (6)
C112	0.1115 (8)	−0.371 (1)	0.2593 (7)
C113	0.0364 (7)	−0.387 (2)	0.2112 (8)
C120	0.3133 (6)	−0.055 (1)	0.4254 (6)
C121	0.3489 (7)	0.079 (1)	0.4757 (7)
C122	0.4121 (8)	0.031 (2)	0.5335 (8)
C123	0.4516 (9)	0.144 (2)	0.5862 (9)
C130	0.1753 (6)	0.061 (1)	0.3929 (6)
C131	0.1649 (6)	−0.027 (1)	0.4562 (6)
C132	0.1127 (7)	0.054 (2)	0.4887 (7)
C133	0.0978 (7)	−0.023 (2)	0.5541 (7)
C210	0.2930 (6)	−0.232 (1)	0.1871 (6)
C211	0.3619 (7)	−0.229 (1)	0.2459 (8)
C212	0.3827 (9)	−0.395 (2)	0.2679 (10)
C213	0.4407 (10)	−0.436 (2)	0.2730 (12)
C220	0.1817 (7)	−0.100 (1)	0.0800 (7)
C221	0.1507 (7)	0.026 (1)	0.0282 (6)
C222	0.0844 (8)	−0.039 (2)	−0.0354 (7)
C223	0.0512 (8)	0.080 (2)	−0.0857 (8)
C230	0.3234 (6)	0.011 (1)	0.1069 (6)
C231	0.3289 (9)	−0.092 (2)	0.0447 (8)
C232	0.3907 (8)	−0.041 (3)	0.0165 (8)
C233	0.4321 (13)	−0.101 (3)	0.0145 (21)

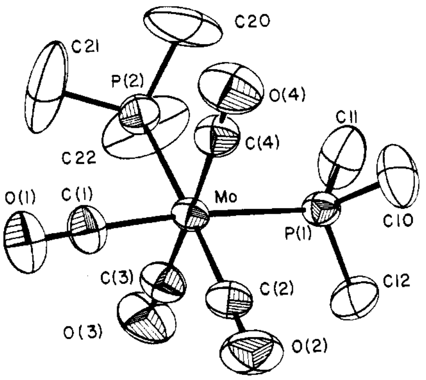

Figure 1. ORTEP picture of the *cis*-$Mo(CO)_4(PMe_3)_2$ molecule, **1**. Each atom is represented by its ellipsoid of thermal vibration scaled to enclose 35% of the electron density, and the atomic numbering scheme is defined.

Results

The molecular structure of *cis*-$Mo(CO)_4(PMe_3)_2$ (**1**) is presented in Figure 1 as an ORTEP diagram. The relevant bond distances and bond angles based on the atomic numbering scheme in this figure are listed in Table V. The most striking dimension is the P(1)–Mo–P(2) angle, which is surprisingly large at 97.54 (4)° and implies a considerable steric interaction between the PMe_3 ligands. The Mo–P bond distances average 2.522 [1] Å, which is similar to the W–P distance in $W(CO)_5(PMe_3)$,[13] 2.516 (2) Å.

As expected, the two types of carbonyl ligands have different Mo–C distances. The CO groups trans to the PMe_3 groups are closer to the metal center at distances of 1.966 (5) and 1.975 (5) Å while the CO ligands cis to the phosphines are bound at 2.022 (6) and 2.042 (5) Å. The steric relationship of the PMe_3 ligands does affect to some extent the geometry of the $Mo(CO)_4$ moiety. The C(1)–Mo–C(2) angle of 88.2 (2)° is slightly compressed from 90°. However, most of the large deviation from a right angle for the P–Mo–P angle is compensated by the P(1)–Mo–C(2) angle of 85.0 (2)°. The remaining dimensions of the $Mo(CO)_4$ group and those pertaining to the PMe_3 ligands are entirely normal. We should mention, though, that there is a rotational disorder (2/1) in one PMe_3 group, if only for the reason that this is the only case in all of the studies that we have performed that any disorder has been detected.

The molecular structure of *cis*-$Mo(CO)_4(PEt_3)_2$ (**2**) and an atomic labeling scheme are given in Figure 2. The structural dimensions are very similar to those found for **1**, and most of the differences can be ascribed to the larger steric bulk of the PEt_3 ligand. The bond distances and angles presented in Table VI support this idea. First, the P(1)–Mo–P(2) angle has increased to 100.27 (3)° and the M–P bond distances average 2.544 (4) Å, indicating that the increase in strain is reduced

Table V. Bond Distances (Å) and Angles (Deg) for *cis*-$Mo(CO)_4(PMe_3)_2$

Mo-P(1)	2.522 (1)	P(1)-C10	1.854 (6)
-P(2)	2.522 (1)	-C11	1.851 (6)
-C(1)	1.966 (5)	-C12	1.848 (5)
-C(2)	1.975 (5)	P(2)-C20	1.83 (1)
-C(3)	2.022 (6)	-C21	1.79 (1)
-C(4)	2.042 (5)	-C22	1.78 (1)
C(1)-O(1)	1.144 (5)	-C23	1.82 (2)
C(2)-O(2)	1.142 (5)	-C24	1.84 (2)
C(3)-O(3)	1.140 (6)	-C25	1.76 (2)
C(4)-O(4)	1.125 (6)		
P(1)-Mo-P(2)	97.54 (4)	Mo-P(1)-C10	114.1 (2)
-C(1)	173.2 (2)	-C11	123.1 (2)
-C(2)	85.0 (2)	-C12	112.3 (2)
-C(3)	90.5 (2)	C10-P(1)-C11	101.2 (4)
-C(4)	90.8 (1)	-C12	102.6 (3)
P(2)-Mo-C(1)	89.3 (2)	C11-P(1)-C12	100.9 (4)
-C(2)	177.4 (2)	Mo-P(2)-C20	115.7 (6)
-C(3)	88.5 (2)	-C21	116.4 (5)
-C(4)	89.9 (2)	-C22	118.3 (5)
C(1)-Mo-C(2)	88.2 (2)	C20-P(2)-C21	98 (1)
-C(3)	89.4 (2)	-C22	99.8 (9)
-C(4)	89.6 (2)	C21-P(2)-C22	104 (1)
C(2)-Mo-C(3)	91.8 (2)	Mo-P(2)-C23	109.8 (9)
-C(4)	90.4 (2)	-C24	111.9 (8)
C(3)-Mo-C(4)	177.5 (2)	-C25	126.7 (9)
Mo-C(1)-O(1)	176.8 (5)	C23-P(2)-C24	103 (2)
-C(2)-O(2)	179.0 (5)	-C25	99 (2)
-C(3)-O(3)	178.0 (6)	C24-P(2)-C25	103 (2)
-C(4)-O(4)	178.2 (5)		

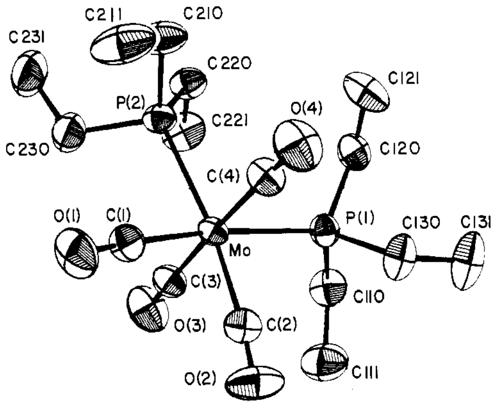

Figure 2. ORTEP picture of the *cis*-$Mo(CO)_4(PEt_3)_2$ molecule, **2**. Each atom is represented by its ellipsoid of thermal vibration scaled to enclose 35% of the electron density, and the atomic numbering scheme is defined.

---

(13) Cotton, F. A.; Darensbourg, D. J.; Kolthammer, B. W. S. *Inorg. Chem.* **1981**, *20*, 4440.

Table VI. Comparative Bond Distances (Å) and Angles (Deg) for *cis*-$Mo(CO)_4L_2$ ($L = PEt_3$ (2) or $P(n\text{-}Bu)_3$ (3))

	2	3
Mo-P(1)	2.541 (1)	2.546 (2)
-P(2)	2.546 (1)	2.558 (2)
-C(1)	1.977 (4)	1.96 (1)
-C(2)	1.977 (4)	1.96 (1)
-C(3)	2.028 (4)	1.99 (1)
-C(4)	2.035 (4)	1.99 (1)
C(1)-O(1)	1.152 (5)	1.140 (9)
C(2)-O(2)	1.144 (5)	1.14 (1)
C(3)-O(3)	1.139 (4)	1.17 (1)
C(4)-O(4)	1.140 (5)	1.18 (1)
P(1)-C110	1.836 (5)	1.834 (8)
-C120	1.836 (4)	1.796 (9)
-C130	1.831 (5)	1.844 (9)
P(2)-C120	1.843 (5)	1.891 (9)
-C220	1.839 (4)	1.87 (1)
-C230	1.840 (5)	1.853 (9)
P(1)-Mo-P(2)	100.27 (3)	99.29 (9)
-C(1)	172.1 (1)	173.0 (3)
-C(2)	87.1 (1)	86.6 (3)
-C(3)	89.5 (1)	92.4 (3)
-C(4)	86.9 (1)	91.1 (3)
P(2)-Mo-C(1)	87.4 (1)	87.7 (3)
-C(2)	172.1 (1)	173.4 (3)
-C(3)	88.6 (1)	88.3 (3)
-C(4)	91.8 (1)	92.8 (3)
C(1)-Mo-C(2)	85.3 (2)	86.5 (4)
-C(3)	92.7 (2)	88.9 (4)
-C(4)	91.0 (2)	87.5 (4)
C(2)-Mo-C(3)	88.6 (2)	88.4 (4)
-C(4)	91.5 (2)	90.2 (4)
C(3)-Mo-C(4)	176.4 (2)	176.2 (4)
Mo-C(1)-O(1)	176.4 (4)	179.1 (9)
-C(2)-O(2)	174.6 (4)	177 (1)
-C(3)-O(3)	178.2 (4)	176.3 (9)
-C(4)-O(4)	179.1 (4)	175.5 (9)
Mo-P(1)-C110	116.4 (2)	121.7 (3)
-C120	112.4 (2)	117.2 (3)
-C130	118.1 (2)	110.7 (3)
C110-P(1)-C120	100.5 (2)	97.0 (5)
-C130	102.9 (3)	102.7 (4)
C120-P(1)-C130	102.6 (3)	105.3 (5)
Mo-P(2)-C210	117.9 (2)	121.0 (3)
-C220	111.9 (2)	118.7 (4)
-C230	116.7 (2)	109.5 (3)
C210-P(2)-C220	100.3 (2)	97.6 (5)
-C230	103.6 (3)	102.9 (5)
C220-P(2)-C230	101.8 (2)	104.9 (5)

both by increasing the angle and by removing the triethylphosphine ligands to longer distances from the metal center. The increased steric interaction has also affected the dimensions of the $Mo(CO)_4$ portion of the molecule. There is a significantly smaller C(1)-Mo-C(2) angle of 85.3 (2)° and greater distortion involving the groups CO(3) and CO(4). The P(1)-Mo-C(4) angle of 86.9 (1)° and the P(2)-Mo-C(4) angle of 91.8 (1)° are representative of the tilting of the O(3)···Mo···O(4) axis with respect to the P(1), P(2), Mo, C(1), C(2) plane. This trend was observed to a much larger extent in the structures of the *cis*-$Mo(CO)_4L_2$ ($L = PMe_2Ph$, $PMePh_2$, PPh_3) complexes.[7]

The expected trend in M-C bond distances is observed with averages of 1.977 (1) and 2.032 (5) Å for the CO groups trans and cis to the PEt_3 ligands, respectively.

The triethylphosphine ligands contain no unusual dimensions, with average P-C and C-C bond distances of 1.837 [5] and 1.511 [8] Å and an average P-C-C angle of 115.6 [20]°. The hydrogen atoms are also found at normal positions, and the data concerning these are presented as supplementary material (average $d_{C-H} = 0.95$ Å).

The structure of *cis*-$Mo(CO)_4[P(n\text{-}Bu)_3]_2$ (3) is remarkably similar to the structure of 2. Because of the difficulties encountered in obtaining this structure (outlined in the Experimental Section), the accuracy of the dimensions is somewhat diminished. We should also note that the general effect of the increased thermal motion is to decrease the observed bond distances with respect to those that would be obtained under ideal conditions. This is particularly apparent in the dimensions of the outer reaches of the *n*-butyl chains. Nonetheless, a good representative model for the structure of *cis*-$Mo(CO)_4[P(n\text{-}Bu)_3]_2$ was obtained, and all of the salient features are listed in Table VI. An ORTEP diagram of the molecule is given in Figure 3, where the atomic numbering scheme is also defined.

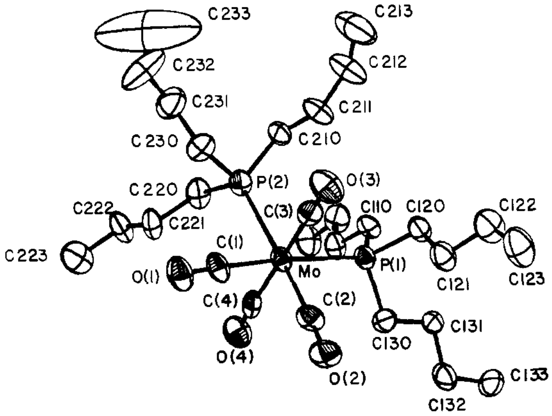

Figure 3. ORTEP picture of the *cis*-$Mo(CO)_4[P(n\text{-}Bu)_3]_2$ molecule, 3. Each atom is represented by its ellipsoid of thermal vibration scaled to enclose 35% of the electron density, and the atomic numbering scheme is defined.

The disposition of the ligands around the metal center in 3 indicates that there are comparably large steric interactions between the PR_3 ligands in 2 and 3 and the effects of the distortion caused by these interactions on the $Mo(CO)_4$ group are similar in the two cases. Notably, the $P(n\text{-}Bu)_3$ groups appear to interact to a greater extent with CO(3) and CO(4) as suggested by the P-Mo-C angles. The results are consistent with the expected trend in M-C binding distances although the uncertainties in these distances preclude any more positive statement on this point.

Discussion

Comparison of the PMe_3, PEt_3, and $P(n\text{-}Bu)_3$ Compounds. Within the group of three *cis*-$Mo(CO)_4(PR_3)_2$ compounds studied here, both the structural and the kinetic trends are those expected from a consideration of the steric requirements of the phosphines. As a gauge of that property we may use Tolman's cone angles,[14] which are 118, 132, and 132° for PMe_3, PEt_3, and $P(n\text{-}Bu)_3$, respectively. Thus, we expect fairly large differences between *cis*-$Mo(CO)_4(PMe_3)_2$ and both of the *cis*-$Mo(CO)_4(PR_3)_2$ compounds with R = Et or *n*-Bu but only minor differences between the latter two. Structurally, this pattern is evident in the P-Mo-P angles, which are 97.5, 100.3, and 99.3°, and also in the Mo-P distances, which are 2.522 (1), 2.544 (4), and 2.552 (8) Å. The increase in the Mo-P distances may be a direct response to the greater steric requirements of the phosphines, in the sense that when the phosphines move away from the metal atom the repulsion between the two phosphines is lessened. It may also be wholly or partly an *in*direct result, in the sense that as the P-Mo-P angle deviates more from 90°, the ability of the Mo atom to form bonds decreases, thus causing the Mo-P bonds to become weaker and hence longer. In any event, the increase in Mo-P distances implies weakening of the bonds, and this should have consequences in the reactivities.

---

[14] Tolman, C. A. *Chem. Rev.* 1977, *77*, 313.

Table VII. Comparative Rate and Equilibrium Parameters for the Intramolecular Isomerization of $Mo(CO)_4(PR_3)_2$ Derivatives at 64.8 °C

R	10^4k_1, s^{-1}	$t_{1/2}$, min	k_1/k_{-1}	ΔG, kcal mol^{-1}
Me	0.084	1375	0.62	0.32
Et[a]	2.10	55.0	7.0	−1.30
n-Bu[a]	1.67	69.2	5.3	−1.12

[a] Data were taken from ref 4.

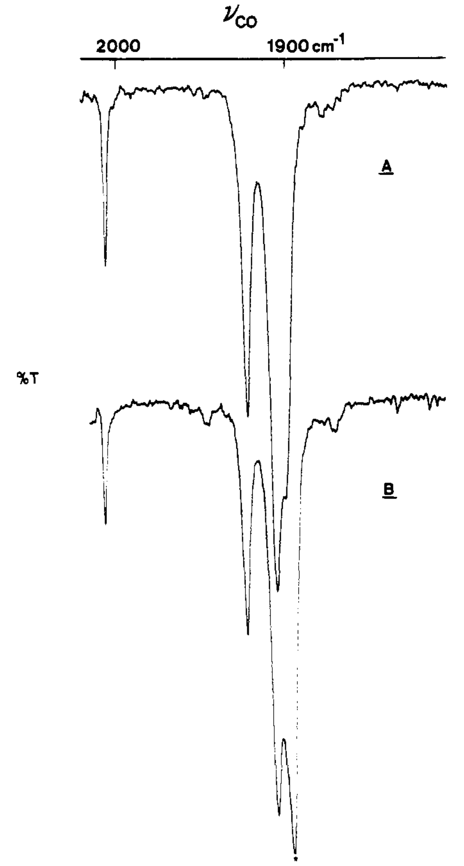

Figure 4. Infrared spectra of $Mo(CO)_4(PMe_3)_2$ in heptane: (A) pure *cis*-$Mo(CO)_4(PMe_3)_2$ complex bands (2019 cm^{-1}) $A^{(2)}$, (1922) $A_1^{(1)}$, (1905) B_1, and (1899) B_2; (B) equilibrium *cis-/trans*-$Mo(CO)_4(PMe_3)_2$ distribution at 64.8 °C. The peak at 1895 cm^{-1} marked by an asterisk is due to the trans species.

As noted in the Introduction the *cis*-$Mo(CO)_4(PR_3)_2$ (R = Et, *n*-Bu) derivatives have already been shown to undergo thermally activated isomerization via an intramolecular, nondissociative process in solution (eq 1) to an equilibrium cis/trans mixture.[4] In the present study, qualitatively analogous behavior was observed for the *cis*-$Mo(CO)_4(PMe_3)_2$ species in solution but with notable differences in the rate of approach to equilibrium and the isomer distribution at equilibrium. Data for all three systems are summarized in Table VII. Figure 4 displays the infrared spectral traces in the ν(CO) region of *cis*-$Mo(CO)_4(PMe_3)_2$ and the resulting *cis-/trans*-$Mo(CO)_4(PMe_3)_2$ mixture obtained upon thermal isomerization at 64.8 °C. The data summarized in Table VII for the *cis*-$Mo(CO)_4(PR_3)_2 \rightarrow$ *trans*-$Mo(CO)_4(PR_3)_2$ isomerization reactions reveal the anticipated trend as a function of the steric bulk of the trialkylphosphine ligand. That is, the smaller PMe_3 ligand favors the cis stereochemistry slightly (ΔG for reaction 1 being 0.32 kcal mol^{-1}), which minimizes the number of mutually trans CO groups. Concomitantly the rate of cis → trans isomerization is much slower than that for the corresponding process involving the PEt_3 and $P(n\text{-}Bu)_3$ species. The kinetic observations are directly compatible with the structural results, where a greater distortion toward the trans disposition of the phosphine ligands is seen in the ground-state structures of the *cis*-$Mo(CO)_4(PR_3)_2$ (R = Et, *n*-Bu) derivatives. Preliminary results on the *cis*-$Cr(CO)_4(PMe_3)_2$ species, where significantly greater distortions from ideal octahedral geometry are expected, indicate the trans stereochemistry to be favored with $K_{eq} \approx 1.7$ at 32 °C and the cis → trans isomerization rate to have a $t_{1/2}$ value <15 min.[15] On the other hand, $Cr(CO)_4(PEt_3)_2$ exists predominantly in the trans isomeric form.[15]

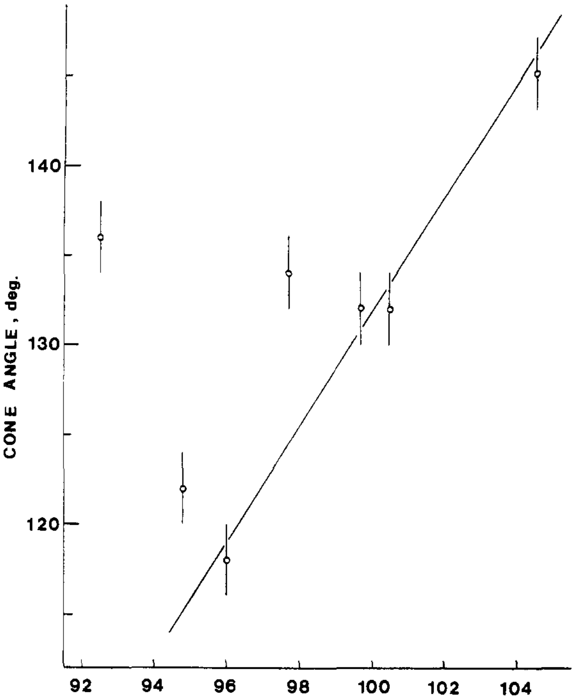

Figure 5. Plot of P–Mo–P angles vs. phosphine cone angles for the seven compounds listed in Table VIII.

Comparison of *cis*-$Mo(CO)_4L_2$ Structures More Generally. We now have structural and reactivity data for seven compounds of the type *cis*-$Mo(CO)_4(PR_3)(PR'_3)$. In addition to compounds **1**–**3**, for which the structures are reported here, we have previously described the structures of the compounds containing $(PMe_2Ph)_2$ (**4**), $(PMePh_2)_2$ (**5**), $(PPh_3)_2$ (**6**), and $(PMe_2Ph)(PPh_3)$ (**7**). Table VIII presents a summary of the pertinent structural data. When we examine the data for this entire set of compounds, it is quickly evident that there are some seeming irregularities.

As we have noted and discussed previously, compound **6** with its cis PPh_3 groups is in some ways in a class by itself, exhibiting several distortions (e.g., in the P(1)–Mo–C(1), P(2)–Mo–C(4), and C(1)–Mo–C(2) angles) that are markedly different from those in the other compounds. Evidently the exceptionally large steric demand made by two cis PPh_3 ligands, as also evidenced by the very large P–Mo–P angle of 104.62°, leads to effects that are qualitatively and not just quantitatively different from those in the other molecules. This is true of the reactivity as well, since **6** undergoes unimolecular dissociative loss of a phosphine ligand at least 3 orders of magnitude more rapidly than any of the others.

Even among the six remaining compounds, there is one structural feature that appears to behave in an unaccountable manner. This parameter is none other than the one that might have been expected to show the most direct dependence of the steric demands of the phosphine ligands, namely, the P–Mo–P

---

(15) Darensbourg, D. J.; Sachs, R., unpublished observations.

Table VIII. Some Bond Lengths (Å) and Angles (Deg) in a Series of Seven *cis*-$Mo(CO)_4(PR_3)_2$ Compounds

	PR_3						
	PMe_3 (**1**)	PEt_3 (**2**)	P(*n*-Bu)$_3$ (**3**)	PMe_2Ph (**4**)	$PMePh_2$ (**5**)	PPh_3 (**6**)	PMe_2Ph, PPh_3 (**7**)
Mo-P (av)	2.522 (1)	2.544 (4)	2.552 (8)	2.529 (5)	2.555 (14)	2.577 (2)	2.562 (1) 2.538 (1)
Mo-C(trans)	1.971 (6)	1.977 (1)	1.96 (1)	1.982 (3)	1.978 (4)	1.972 (2)	1.977 (3)
Mo-C(cis)	2.032 (14)	2.032 (5)	1.99 (1)	2.016 (18)	2.027 (7)	2.040 (19)	2.034 (3)
M-C(cis) – M-C(trans)	0.061 (15)	0.055 (5)	0.03 (2)	0.034 (18)	0.049 (8)	0.068 (19)	0.054 (5)
P-Mo-P	97.54 (4)	100.27 (3)	99.29 (9)	94.78 (5)	92.52 (5)	104.62 (7)	97.73 (2)
P(1)-Mo-C(1)	173.2 (2)	172.1 (1)	173.0 (3)	175.5 (2)	178.5 (2)	163.7 (2)	173.33 (9)
-C(2)	85.0 (2)	87.1 (1)	86.6 (3)	87.1 (2)	92.9 (2)	80.6 (2)	89.4 (1)
P(2)-Mo-C(1)	89.3 (2)	87.4 (1)	87.7 (3)	89.7 (2)	87.8 (2)	91.7 (2)	87.8 (1)
-C(2)	177.4 (2)	172.1 (1)	173.4 (3)	176.3 (2)	172.2 (2)	173.2 (2)	172.8 (1)
P(1)-Mo-C(3)	90.5 (2)	89.5 (1)	92.4 (3)	89.3 (2)	90.6 (2)	94.0 (2)	93.85 (8)
-C(4)	90.8 (1)	86.9 (1)	91.1 (3)	87.8 (2)	88.9 (2)	90.3 (2)	87.51 (8)
P(2)-Mo-C(3)	88.5 (2)	88.6 (1)	88.3 (3)	94.0 (2)	88.8 (2)	90.6 (2)	90.38 (8)
-C(4)	89.9 (2)	91.8 (1)	92.8 (3)	87.0 (2)	95.8 (2)	84.4 (2)	87.10 (9)
C(1)-Mo-C(2)	88.2 (2)	85.3 (2)	86.5 (4)	88.4 (3)	86.9 (3)	83.0 (3)	85.0 (1)

angle. Figure 5 shows a plot of P–Mo–P angles vs. the cone angles. In the case of the mixed-ligand species we use the mean of the two cone angles. Uncertainty intervals of ±2° in the cone angles, as suggested by Tolman, have been indicated. There is clearly no simple relationship among all the points as plotted. We do note, however, that if only the four compounds in which both phosphine ligands have three identical R groups, **1**, **2**, **3**, and **6**, are considered, there is an approximately linear relationship. The other three compounds all deviate from this line in the sense of seeming to make a steric demand much smaller than the cone angle would imply.

This can be accounted for, at least in part, by recognizing that for a phosphine with a mixed set of R groups the cone angle is not unambiguously defined. To speak specifically in terms of the present cases, the steric requirements of CH_3 and C_6H_5 groups are quite different and merely averaging them does not necessarily provide a meaningful parameter for use in the present discussion, because rotations about both of the Mo–P bonds can lead to large variations in the repulsive forces between the two mutually cis phosphines. The simplest, but doubtless only approximate, way to take this factor into account is to recognize that there are orientations that will reduce the "effective" cone angles of the PMe_nPh_{3-n} ligands, as experienced by each other, to values much lower than those used in Figure 5. In other words, the points for **4** and **5** could be lowered appreciably, the limit being set (probably) by the cone angle of PMe_3. This would put the points for these two compounds, especially that for **4**, fairly close to the line. For **7**, however, this procedure would give only a slight lowering (ca. 2°, to the bottom of its error bar), thus leaving it still quite high.

There are probably steric factors other than those gauged by the cone angle criterion alone that are relevant here, and there may well be some essentially electronic effects operating as well. Perhaps the most useful summarizing statement that can be made is the following. Steric requirements of the ligands in *cis*-$M(CO)_4L_2$ compounds have a major role in determining their structural and kinetic characteristics, but there are aspects of this steric problem—and perhaps other factors as well—that are not satisfactorily covered by crude arguments based on purely geometrical criteria.

One final observation may be made about Figure 5. We may estimate the cone angle at (or below) which a P–Mo–P angle of 90° could be expected, by extrapolation using the line through the data for **1**–**3** and **6**. The value so obtained is 99.5°. According to Tolman's tables[14] the following phosphines (with their cone angles in parentheses) might be suitable: PH_3 (87°), $P(OCH_2)_3CR'$ (101°), and PH_2Ph (101°). It is also pertinent to note that CO itself, with a cone angle estimated to be <113° and probably about 95°, which, of course, gives 90° L–Mo–L angles in $Mo(CO)_6$, is consistent with that extrapolation.

Acknowledgment. This work was supported by the National Science Foundation. D.J.D. thanks Tulane University for sabbatical leave during the Spring semester, 1980. B.W.S.K. was the recipient of a NATO postdoctoral fellowship administered by the Natural Sciences and Engineering Research Council of Canada, 1979–1981.

Registry No. **1**, 16027-45-5; **2**, 19217-80-2; **3**, 16244-54-5.

Supplementary Material Available: A listing of structure factors for compounds **1**–**3** and tables of thermal parameters for all atoms, positional and thermal parameters for hydrogen atoms in **2**, and C–C distances in **2** and **3** (35 pages). Ordering information is given on any current masthead page.